Eur. Phys. J. B **10**, 197–200 (1999)

THE EUROPEAN PHYSICAL JOURNAL B

EDP Sciences

Rapid Note

Origin and doping dependence of the photoemission pseudogap in Cu oxides

M.D. Núñez-Regueiro[a]

Grenoble High Magnetic Field Laboratory, MPI-FKF and CNRS, BP 166, 38042 Grenoble, France

Received 9 April 1999

Abstract. A recent report on ARPES on insulating $Ca_2CuO_2Cl_2$, compared to previous data from $Sr_2CuO_2Cl_2$ and Dy-doped $Bi_2Sr_2CaCu_2O_{8+\delta}$, sheds new light on the origin of the anisotropic pseudogap observed in the normal state of underdoped cuprate oxides. The energy dispersion of the insulator is attributed to strong AF correlations enhanced by the diagonal hopping between magnetic sites, which is progressively deformed by the possibility of nearest neighbour hopping, that increases with hole doping.

PACS. 74.25.Jb Electronic structure – 74.72.-h High-T_c compounds

In a recent paper, Ronning *et al.* [1] reported a challenging angle resolved photoemission (ARPES) study on $Ca_2CuO_2Cl_2$, a parent compound of high-T_c superconductors. From their analysis they argue the existence of a Fermi surface remnant, even though the system is a Mott insulator. Furthermore the lowest energy peak exhibits a dispersion with approximately the $|\cos k_x - \cos k_y|$ form along the $X = (\pi, 0) \rightarrow Y = (0, \pi)$ direction. Together with previous data from insulating $Sr_2CuO_2Cl_2$ [2–4] and from metallic Dy-doped $Bi_2Sr_2CaCu_2O_{8+\delta}$ (Bi2212) [5,6], these results strongly suggest that this d-wave like dispersion for the insulator is the underlying reason for the pseudogap in the underdoped regime. The authors arrive to the fundamental question: "what does the data fitting the nontrivial $|\cos k_x - \cos k_y|$ function so well mean?" [1].

The basic phenomenology of the normal state pseudogap has been now established from different ARPES experiments [1–6]. Two energy scales have been identified in the spectra: a leading edge shift of 20−25 meV and a high-energy hump at 100−200 meV [5], which are referred as the low- and high-energy pseudogaps, respectively [1]. Both, like the superconducting gap have an angular dependence consistent with a d-wave form. The fact that the high-energy pseudogap correlates with the low-energy one which is likely to be related to superconductivity, suggests to Ronning *et al.* [1], that it is likely that the same physics that controls the d-wave dispersion of the insulator is responsible for the d-wave-like normal state pseudogap and the d-wave superconducting gap in the doped samples.

Several models have been proposed for the pseudogap: preformed pairs and phase fluctuations, damped spin-density wave (SDW), resonant valence bond singlet formation and spin-charge separation [7]. Using for the discussion a phenomenological tight-binding approach, shown to describe relevant numerical calculations when they exist, we stress here that the nearly (not exactly) d-wave-like dispersion observed for the insulator can be accounted for by the strong antiferromagnetic (AF) correlations present in the CuO square lattice of these systems. Furthermore, because it is not a nesting effect, this explanation remains valid in the underdoped metallic case. The magnitude of this quasiparticle dispersion is enhanced by the additional (diagonal) hopping between second neighbours Cu sites. With increasing hole concentration the hopping between nearest neighbour (n.n.) sites becomes possible but the influence of these strong local correlations is still important, and the evolution from the insulator to the optimal doped compound is done in a continuous manner. Then we also show that, as proposed by Ronning *et al.* [1], the peculiar energy dispersion of the insulator can be at the origin of the high-energy gap in the underdoped samples.

A key feature in our approach is the presence of a narrow quasiparticle band, distinguished from the incoherent part of the spectrum, and its crossing by the chemical potential. We quote numerical calculations, both in the $t - J$ [8] and the Hubbard models [9], and the experimental behaviour in the normal state, as supporting this approximation.

Weak coupling limit

In a square lattice with n.n. hopping t, on-site Coulomb repulsion U and one electron (or hole) per site, the original band splits due to the AF ordering of the system.

[a] e-mail: nunezreg@labs.polycnrs-gre.fr

The energy dispersion is:

$$\epsilon(k) = \pm\sqrt{2t(\cos k_x + \cos k_y)^2 + V^2}, \quad (1)$$

V being the mixing term between both sublattices. The peaked dispersion centered at $M' = (\pi/2/, \pi/2)$ in the $\Gamma = (0,0) \rightarrow M = (\pi,\pi)$ direction reflects the AF ordering, $\epsilon(X) = \epsilon(M')$, and there is no dispersion at all in the $X \rightarrow Y$ direction for **k**-independent V. In the mean field SDW approximation [10], in the large $U/t \gg 1$ limit, $\Delta \simeq U/2$ and $J = 4t^2/U$, so equation (1) becomes:

$$\epsilon(k) = \pm[\Delta + J(\cos k_x + \cos k_y)^2)] \quad (2)$$

with the same flat behaviour in the $X \rightarrow Y$ direction. In this case the half filling factor is crucial: the gap rapidly closes with doping, that destroys the nesting condition.

Strong coupling limit

These previous approximations fail in the strong coupling case, where, from the beginning, other methods must be used in order to obtain reliable results. The points of Figure 1 correspond to the simulations by Dagotto *et al.* [11] for the 2D $t-J$ model, using a Green function Monte Carlo (GFMC) method, for clusters of different sizes, and $J/t = 0.4$. These results are of general character, *i.e.* independent of the details of the many different studies derived from the Hubbard model. The curve shows that the two first terms describing the hopping of a hole that avoids disturbing the AF background:

$$\epsilon(k) = C - 2\widetilde{t}(\cos 2k_x + \cos 2k_y) - 4\widetilde{t}\cos k_x \cos k_y \quad (3)$$

account for the main contribution to the energy dispersion. The effective hopping $\widetilde{t}$ is the same for both terms. We take $C = -1.25t$ and we plot in Figure 1, equation (3), with $|\,\widetilde{t}\,| = 0.1t$ (with negative sign as in Fig. 1 of Ref. [11]), in order to reproduce the numerical bandwidth. The energies of the different $\boldsymbol{k}$-points can now be easily calculated, to verify the properties already pointed out for this case [11]:

- the minimum energy is obtained at the M' point, $\epsilon(M') = C - 4\widetilde{t}$. The energy of the X point being $\epsilon(X) = C$, the difference between these two minima, $\epsilon(X) - \epsilon(M') = 4\widetilde{t}$ is small, as $\widetilde{t}$ is already a reduced parameter. This point will be in conflict with the experimental results for the undoped cuprate oxides,
- the total bandwidth, $W = 12\ |\widetilde{t}|$, compared to the numerical results of Figure 1 implies:

$$\widetilde{t}/t = \alpha(J/t) \quad (4)$$

  with $\alpha \simeq 1/4$. This value is slightly larger than the more general expression $\alpha \simeq 0.183$, derived from [12], considering $W/t = 2.2(J/t)$ for $J/t < 0.7$,
- a remarkable feature is the almost flat region around the X point, $\epsilon(\pi,\pi/2) = \epsilon(\pi,0) = \epsilon(\pi/2,0) = C$, due to AF correlations,
- but we note that a crucial difference with the previous weak coupling case is the significant energy dispersion in the $X \rightarrow Y$ diagonal, to which both terms in equation (3) contribute. This appears as a signature of the strong coupling limit. Although this direction has not been considered in [11], this main point is confirmed by GFMC simulations for other parameters, *e.g.* [13].

We see from Figure 1 that equations (3, 4) have the sufficient precision (note the better agreement with larger size cluster calculations) to be advantageously used to study the effect on the spectrum of contributions of other origin. In particular, we will use them in the underdoped case, where these strong correlations persist due to the local AF environment, even in the absence of nesting features.

Insulating cuprates

Wells *et al.* [2] first reported an ARPES study on insulating $Sr_2CuO_2Cl_2$. Since this layered copper oxide is particularly difficult to dope, it precisely corresponds to the theoretical scenario of a single hole in the quantum AF background of the cuprates. Therefore it provided a unique opportunity to test calculations, see Figure 2, which yielded to the following conclusions:

- the 2D $t-J$ model describes properly the data along the $\Gamma \rightarrow M$ diagonal, with the highest energy in the valence band for M', as expected from many calculations [8–14],
- the experimental bandwidth is very close to the reduced bandwidth obtained for one hole in an AF background by various techniques; this is in contrast with local density band calculations. The value $W = 0.036$ eV implies in our approach $\widetilde{t} = 0.03$ eV, yielding the dashed curve plotted in Figure 2, which also shows the disagreement with experiment: the observed $X \rightarrow \Gamma$ direction has smaller dispersion than the calculated one, the contrary occurs from $X \rightarrow Y$.

These differences showed the necessity of taking into account further contributions to the diagonal hopping term [13], as had been pointed out long time before [15]. This additional t' term in equation (5), that has been attributed to the overlap of n.n. oxygen atoms, can be derived from the three-band Hubbard Hamiltonian [16], and has different sign depending on the doping carriers [17]: electrons or holes. On the other hand, Andersen *et al.* [18] have pointed out the crucial contribution of Cu4*s* orbitals to this term. The energy dispersion becomes:

$$\epsilon(k) = C - 2\widetilde{t}(\cos 2k_x + \cos 2k_y) - 4(\widetilde{t} + t')\cos k_x \cos k_y \quad (5)$$

with $t' > 0$ for the hole doping case (as done by the photoemission process). In Figure 2 the continuous curve shows how this t' term modifies the $t-J$ spectrum. More structure appears in the $X \rightarrow \Gamma$ direction and $\epsilon(X)$ becomes lower than $\epsilon(\Gamma)$ for $|t'| > \widetilde{t}$, therefore the bandwidth is given by $W = 4(\widetilde{t} - t')$. The maximum in

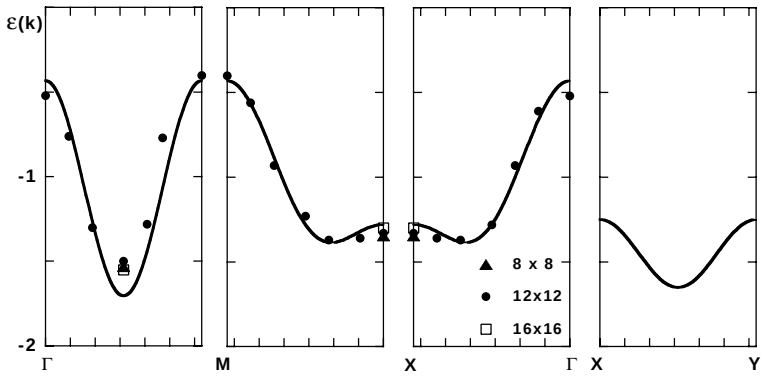

Fig. 1. ϵ *vs.* **k** for the $t-J$ model. The points correspond to the GFMC numerical calculations of [11], for $J/t = 0.4$ and the indicated cluster sizes. The energy unit is t. The continuous curve is given by equations (3, 4).

this direction that for the $t-J$ model was at $k=(\pi/4,0)$ shifts towards $k=(\pi/2,0)$. The effective expression used for the $t-J$ model allows us to determine the optimal t' from equation (5), that fits the experimental data better than in [13]. The $\Gamma \to M$ and $X \to Y$ directions are well described, with the correct bandwidth. In the $X \to \Gamma$ direction, $|t'| > \widetilde{t}$ allows to reproduce $\epsilon(X) \ll \epsilon(M')$ even though the dispersion W' becomes twice the one reported by Wells *et al.* [2]. However, latter measurements on this compound [3] showed that when polarisation effects are carefully taken into account, the dispersion is in very good agreement with our curve: both, the $X \to \Gamma$ bandwidth W' and the position of the maximum, as can be seen in Figure 2.

Although the new data on $Ca_2CuO_2Cl_2$ are consistent with these results from $Sr_2CuO_2Cl_2$, the improved spectral quality allowed Ronning *et al.* [1] to derive further conclusions: there is a remnant Fermi surface in the insulator and the strong correlation effect deforms this otherwise isoenergetic contour (the noninteracting Fermi surface) into a form that matches the $|\cos k_x - \cos k_y|$ dependence very well, but with a very high energy scale of 320 meV. Thus a "d-wave"-like dispersive behaviour seems to exist even in the insulator.

In Figure 3 the high-energy "gap" of $Ca_2CuO_2Cl_2$ is plotted as a function of $|\cos k_x - \cos k_y|/2$, like in [1], the straight line shows the d-wave behaviour. In the same figure we have added the points and the continuous curve corresponding to the good fit that we have already obtained for the $X \to Y$ direction of $Sr_2CuO_2Cl_2$. We note that the linear dependence is not perfect: the inset shows the $X \to Y$ dispersion necessary to obtain exact agreement. See the right panel in Figure 2: the data and the calculation seem to deviate from the theoretical d-wave dispersion. Also the $Ca_2CuO_2Cl_2$ points show some differences, specially for small values of $|\cos k_x - \cos k_y|/2$.

In our calculation the dispersion in the $X \to Y$ direction is a consequence of strong AF correlations in the square geometry of the CuO_2 planes.

Hole doped case

When the parent compound is doped, one expects an increasing probability of hopping to n.n. (although renormalized, $t_{\rm R}$) at expenses of the AF correlations. In our

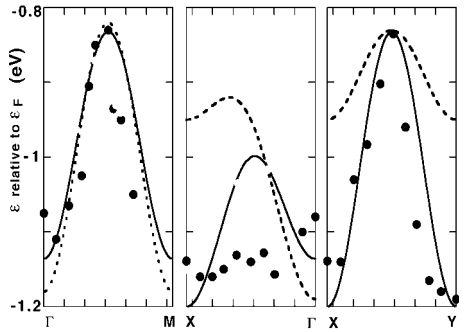

Fig. 2. Comparison of the experimental ϵ *vs.* **k** dispersion for insulating $Sr_2CuO_2Cl_2$ with the calculation for the $t-J$ model (dashed line, Eqs. (3, 4)). Filled circles: data from [2], open circles: data from [3]. The continuous curve is given by equation (5), with $C=-1$ eV, $\widetilde{t}=0.042$ eV, $t'=-0.05$ eV.

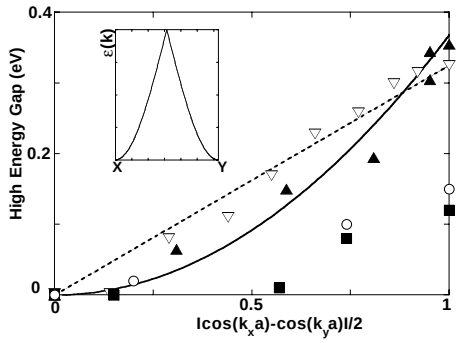

Fig. 3. The "gap" *vs.* $|\cos k_x - \cos k_y|/2$. Dashed line: d-wave line for $Ca_2CuO_2Cl_2$ (empty triangles) as in [1]. Continuous curve: our fit in the right panel of Figure 2 for $Sr_2CuO_2Cl_2$ (filled triangles). Bi2212 data from [1], open circles: 65 K, filled squares: 25 K samples. Inset: $X \to Y$ dispersion necessary to obtain a perfect straight line.

picture, because these interactions are a strong local environment effect, we can consider that it is the relative weight of both processes that changes progressively with doping. The effective dispersion becomes:

$$\epsilon(k) = C - 2t_{\rm R}(\cos k_x + \cos k_y) - 2\widetilde{t}(\cos 2k_x + \cos 2k_y) - 4(\widetilde{t}+t')\cos k_x \cos k_y. \quad (6)$$

This expression allows to describe the evolution observed for Dy-doped Bi2212 samples in [5], as it is shown in Figure 4, see effective parameters in the figure caption. With increasing hole doping the remarkable **k**-dependence in

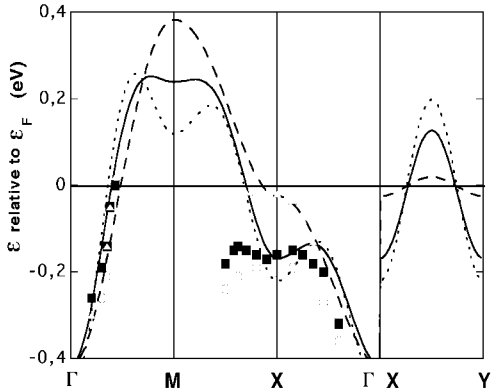

Fig. 4. ϵ *vs.* **k** for Dy-doped Bi2212 samples from [5]. There are no experimental points along $X \to Y$. Dashed-curve: $t_{\rm R} = 0.1$ eV, $\widetilde{t} = 0.005$ eV, $t' = -0.006$ eV for $\sim$ optimal $T_{\rm c} = 85$ K (triangles); continuous curve: $t_{\rm R} = 0.082$ eV, $\widetilde{t} = 0.032$ eV, $t' = -0.042$ eV, for underdoped $T_{\rm c} = 65$ K (squares); and dotted line: $t_{\rm R} = 0.075$ eV, $\widetilde{t} = 0.05$ eV, $t' = -0.055$ eV, for strongly underdoped $T_{\rm c} = 25$ K (open circles), calculated with equation (6).

the $X \to Y$ direction persists, however the magnitude of the gap decreases. (Because there is an energy scale shift between the data in Refs. [1,5] for the same samples, we just include the experimental points in Fig. 3. They have the same $X \to Y$ dependence than our calculated curves in Fig. 4). When the gap closes, the usual dispersion of the n.n. tight-binding case is recovered, this occurs close to optimal doping. In fact, for the 85 K case of Figure 4, a better fit is obtained for very weak but not vanishing AF correlations. The $\Gamma \to M'$ direction is less affected by doping. Along the $X \to M \to M'$ direction the experimental situation is controversial: no clear crossing of the Fermi level has been detected in the pseudogap regime, and shadow bands (points with weaker intensity in the $M' \to M$ direction) have been only reported in [3]. This last situation will imply in our approach even larger values of $\widetilde{t}$ and t', which will better describe the flattening of the band around X. However, points from the same reference [5] for underdoped argon annealed samples seem to go up towards the M point. As we cannot calculate the corresponding intensity, we do not discuss further this point. In both cases, the tendency for the parameters and the conclusion concerning the dispersion in the $X \to Y$ direction will be the same.

This behaviour will be naturally obtained for fixed $t_{\rm R}$, $\widetilde{t}$ and t' in a selfconsistent calculation by just changing the hole doping. In fact, this can be inferred from the exact diagonalization calculation by Eder *et al.* [19], which shows a consistent evolution of the spectra $A(\mathbf{k}, w)$ when going from one to two added holes for an equivalent model.

Conclusion

The energy dispersion of insulating parent compounds can be the consequence of strong AF correlations in the planar square lattice of the Cu oxides. We have shown that the **k**-dependence can be described by an effective dispersion considering the reduced hopping of the photoemission hole in one magnetic sublattice. This dispersion is further enhanced in the $X \to Y$ direction by the contribution of a diagonal term, the main origin of which remains controversial. These strong local correlations will survive with hole doping, although their weight will decrease while the n.n. hopping term becomes more important, until the gap closes near optimal doping.

We have shown that the normal state pseudogap can be interpreted as a remnant property of the insulator that continuously evolves with doping, as first pointed out by Laughlin [20], although within a completely different interpretation. While the exact diagonalization study of the $t - t' - t'' - J$ model by Eder *et al.* [19] did not allow for a sufficiently smooth variation of the concentration to map out the experimental doping dependence, it strongly supports this unifying point of view.

The d-wave form of the superconducting gap suggests testing this dependence for the insulator: the data and the calculation reflecting the effect of strong correlations in the square lattice, although not too far from it, seem to show some differences.

Many of the elements used in our discussion have already been mentioned in the literature in other contexts. The analysis of this accumulated knowledge within our simple picture, gives a coherent explanation of the origin, form and doping behaviour of the controversial [7] normal anisotropic high-energy pseudogap.

References

1. F. Ronning *et al.*, Science **282**, 2067 (1998).
2. B.O. Wells *et al.*, Phys. Rev. Lett. **74**, 964 (1995).
3. S. LaRosa *et al.*, Phys. Rev. B **56**, R525 (1997).
4. C. Kim *et al.*, Phys. Rev. Lett. **80**, 4245 (1998).
5. D.S. Marshall *et al.*, Phys. Rev. Lett. **76**, 4841 (1996).
6. H. Ding *et al.*, Nature **382**, 52 (1996); M.R. Norman *et al.*, Nature **392**, 157 (1998) and references therein.
7. A summary of different theories is given in [1]. See also the boson-fermion model by J. Ranninger *et al.*, Phys. Rev. Lett. **80**, 5643 (1998), in the line by M. Randeria *et al.*, `cond-mat/9710223`; the Cooper pair droplets without phase coherence, B.K. Chakraverty, T.V. Ramakrishnan, Phys. C **282-287**, 290 (1997) and the model for pseudogaps by P. Nozières, F. Pistolesi, `cond-mat/9902273`.
8. See review by E. Dagotto, Rev. Mod. Phys. **66**, 763 (1994).
9. R. Preuss, W. Hanke, W. von der Linden, Phys. Rev. Lett. **75**, 1344 (1995); D. Duffy *et al.*, Phys. Rev. B **56**, 5597 (1997).
10. N. Bulut, D.J. Scalapino, S.R. White, Phys. Rev. Lett. **73**, 748 (1994).
11. E. Dagotto *et al.*, Phys. Rev. Lett. **73**, 728 (1994).
12. D. Poilblanc *et al.*, Phys. Rev. B **47**, 14267 (1993).
13. A. Nazarenko *et al.*, Phys. Rev. B **51**, R8676 (1995).
14. Z. Liu, E. Manousakis, Phys. Rev. B **45**, 2425 (1992).
15. M. Hybertsen *et al.*, Phys. Rev. B **41**, 11068 (1990).
16. A.A. Aligia *et al.*, Phys. Rev. B **49**, 13061 (1994).
17. T. Tohyama, S. Maekawa, Phys. Rev. B **49**, 3596 (1994) and references therein.
18. O.K. Andersen *et al.*, J. Phys. Chem. Solids **56**, 1573 (1995), and preprint.
19. R. Eder, Y. Otha, G.A. Sawatzky, Phys. Rev. B **55**, R3414 (1997).
20. R.B. Laughlin, Phys. Rev. Lett. **79**, 1726 (1997).